SOME APPLICATIONS RELATED TO THE STRUCTURAL INTEGRITY ANALYSES OF CANDU 6 PRESSURE TUBES

Vasile S. RADU
Institute for Nuclear Research Pitesti, Romania
Present Address: European Commission, Joint Research Center, IE Petten, Netherlands

ABSTRACT: The flaws found during in-service inspection of Zr-2.5%Nb CANDU pressure tubes include fuel bundle bearing pad fretting flaws and debrise fretting flaws. In-service flaws are evaluated using fitness-for-service procedures to justify continued operation of pressure tube containing the flaw. The flaw evaluation procedures address crack initiation due to Delayed Hydride Cracking (DHC) under constant loading and also address fracture initiation and plastic collapse.The paper presents some applications related to the influence of the residual hoop stresses at roll-expanded joint region into stainless steel fittings at both ends on the structural integrity evaluation in the presence of blunt flaws. Two cases of blunt flaws were considered for evaluation: fuel bundle bearing pad fretting flaws and debrise fretting flaws. The blunt flaw geometry modeling and stress-strain analyses were performed by means finite element method (FEM) with FEA-Flaw computer code. The allowable peak flaw-tip stress and the Failure Assessment Diagram (FAD) for DHC initiation criterion were used for integrity assessment for the mentioned blunt flaws.
Applications are performed as part of the research program address to evaluation of the in-service inspection results of the fuel channels from Cernavoda NPP.

KEYWORDS: CANDU pressure tube, DHC, blunt flaws, residual hoop stress, structural integrity assessment

1. INTRODUCTION

Romania has only one NPP into operation, CANDU 6 type reactor located in the Cernavoda site. At Institute for Nuclear Pitesti a research program for CANDU fuel channels structural integrity assessment is in progress.

In a CANDU 6 reactor the pressure tubes are made from cold-worked Zr-2.5%Nb alloy. A pressure tube has a wall thickness of 4 mm and an inside diameter of 103 mm and is rolled into the end fittings. Over time, these tubes are susceptible to a slow corrosion process, which also leads to a gradual pickup of deuterium in the tubes. When the hydrogen/deuterium concentration exceeds the terminal solid solubility (TSS), the tubes are susceptible to a crack initiation and propagation process called delayed hydride cracking (DHC) [1], [2].

The roll-expansion process induces residual stresses in the pressure tube and the end fittings. The residual stresses in the components affect the performance of the joint and consists of compressive joint stresses (in the roll-expanded region of PT) and transitions stresses that occur between the roll-expanded region and the unaffected region of pressure tube [3]. The transition stresses can be either tensile or compressive. The transition from the rolled region to the unaffected region of the pressure tube is referred to as the burnish mark [4]. There is the potential for DHC initiation in Zr-2.5%Nb pressure tube material when a stress concentration, due to a flaw, is in a region with high applied stress and a hydrogen isotope concentration which exceed the solubility in the alloy. Consequently, the potentially high residual stress levels could exist adjacent to the burnish mark and the major consideration for fretting flaws at rolled joints location is DHC initiation. The flaws found during in-service inspection of Zr-Nb pressure tubes include fuel bundle bearing pad fretting flaws (BPF) and debrise fretting flaws (DFF) [5, 6]. In the present paper both cases of blunt flaws were considered for evaluation: fuel bundle bearing pad fretting flaws and debrise fretting flaws. The blunt flaw geometry modeling and stress-strain analyses were performed by means finite element method (FEM) with FEA-Flaw computer code. The allowable peak flaw-tip stress [4, 7] and the Failure Assessment Diagram (FAD) for initiation of DHC criteria [8, 9, 10] were used for structural integrity assessment for the mentioned blunt flaws.

2. CANDU 6 PRESSURE TUBES STRUCTURAL INTEGRITY

2.1 Residual stresses concern

The following risk factors must be controlled and minimized in order to assure the CANDU pressure tubes structural integrity [14]:presence of hydrides, counting concentrators and preferable cracking orientations, tensile stress as sum of the total stress and its amplification by crack tip, duration of exposure to both previous mentioned risk factors.

The DHC phenomenon is a cracking process requiring hydrogen diffusion to a stress concentrator, followed by nucleation, growth and fracture of hydrides [6, 11, 12]. In a stress gradient generated by of flaw presence in the pressure tube under operating stress (cumulated from internal and residual stresses at rolled joint), hydrogen diffuses to the stress concentrator because of the lowering of the chemical potential of hydrogen due to tensile hydrostatic stress.

The roll-expansion process induces residual stresses in the pressure tube and the end fittings [3, 13]. The total stress in the pressure tube is sum of: i)operating stresses due to internal pressure, and thermal and mechanical loads; ii) residual stresses in the pressure tube induced during fabrication of the pressure tube and roll-expansion process.
The transition stresses resulted from the roll-expanded region can be as hoop stress type in burnish mark zone of the pressure tube. The cold worked Zr-2.5%Nb alloy is anisotropic and the crystallographic structure permits a DHC

behavior enough sensitive to tensile hoop stress. "Over-extension" of joints, resulting from a inadequate axial location of the rollers, could cause high residual hoop stresses in the pressure tube. In the operating temperature range of CANDU pressure tubes, 250-315 °C the design stress is σ_D=160 MPa [14]. The maximum depth of a surface flaw, a_c, that can be tolerated without crack growth by DHC is estimated [14]:

$$a_c = \frac{S \cdot \left(\frac{K_{IH}}{\sigma_D} \right)^2}{1.21 \cdot \pi} \quad (1)$$

where: S ~ 1.5 when the flaw length is three times the flaw depth. With K_{IH} =4.5 MPa.√m the value of a_c is 0.3 mm, providing a margin of four times in regard to rejecting values by 0.075 mm.

In early commercial CANDU reactors constructed before 1975, incorrect roll-expansion procedures produced excessive residual stresses in the pressure tube. At some of rolled joints in these reactors, the residual stresses were sufficiently high to initiate DHC in the pressure tube [13, 15]. If the rolls are advanced too far, part of the pressure tube is deformed without support from the stainless steel and large residual tensile stresses, over 400 MPa (Figure 1, [16]). With the early rolled joints, the residual tensile stresses were up to 700 MPa [14], so a_c would be small ~ 0.016 mm. Consequently, cracks may initiate. Revised roll-expansion procedures have eliminated the high stresses in the pressure tube in the CANDU reactors constructed since 1973 [13]. In reactors that were not yet in service, joints already made were stress relieved 550 °C for 15 min, which reduced the residual stress to below 100 MPa. no DHC has been observed in new rolled joints where the rolling process was modified to ensure the hoop tensile stresses below 100 MPa.

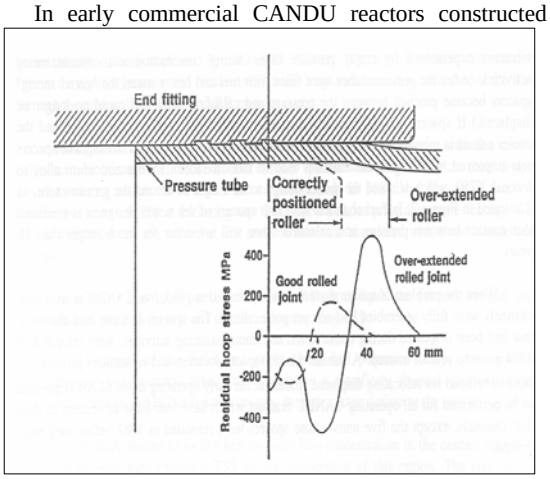

Figure 1. Residual stresses at rolled joint [16]

The example of the structural integrity analyses performed in the present paper will consider the residual stresses values from 50 MPa up to 300 MPa for pressure tube containing a fuel bundle bearing pad fretting flaw (BPF) and a debrise fretting flaw (DFF) under operating stresses due to internal pressure.

2.2 Hydride thermal ratcheting at rolled joints

Many observations of the behavior of hydrogen in zirconium alloys suggested that there is a hysteresis effect concerning to the solubility. This effect depends upon whether hydrides are dissolving or precipitating. These effects have been put in evidence using several techniques: differential scanning calorimetry, measurements of changes in thermal expansion, electrical resistivity, and elastic modulus. In all cases, the effect is manifested as a difference between the concentration of hydrogen in solution in the metal in equilibrium with dissolving hydrides at a particular temperature and the concentration in equilibrium with precipitating hydrides at the same temperature. The hysteresis effect could be explain by means of the internal stresses in the solid zirconium alloys. These internal stresses developed during precipitation and dissolution of hydride caused by the 17% volume change associated with the transformation of alpha zirconium matrix to delta hydride [16]. The internal stresses develop within the system during the alpha zirconium to hydride transformation (and the reverse) and will be more intense near the hydrides themselves and both internal stresses and the plastic work associated with the formation and dissolution of hydrides are responsible for the solubility behavior of hydrogen in zirconium alloys. The thermal cycling of a zirconium

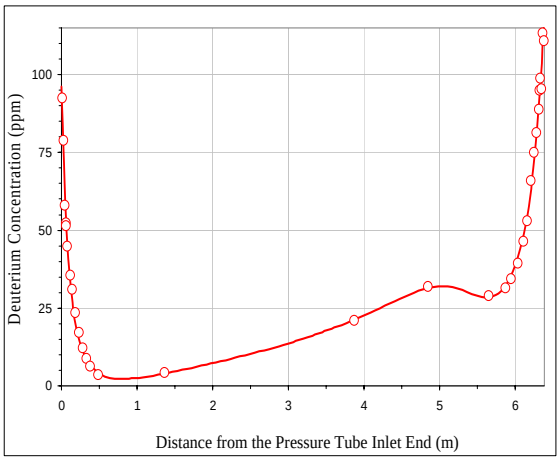

Figure 2. Deuterium concentration along the pressure tube after 17 hot years [18]

sample containing hydrogen can cause large increases in hydride formation at the crack tip. The phenomenon has been called the thermal ratcheting of hydrogen in zirconium alloy [17].

From the structural integrity analyses point of view a main issue is that some tubes in CANDU NPP have sufficient hydrogen isotope concentration in the rolled joints to reach TSSD (Terminal Solid Solubility for hydride Dissolution). In the Figure 2 [18] deuterium concentration along the pressure tube after 17 hot years reached high concentrations in the rolled joint regions. In these conditions the flaws in rolled joint locations will be under hydride ratcheting conditions. Accordingly, the flaw tip hydrides will not be fully dissolved at the operating temperatures and supplementary hydrides generate at the flaws during each thermal cycle. This will likely increase the susceptibility to crack initiation, compared to the non-ratcheting case at lower hydrogen concentration levels in which the flaw tip hydrides are completely dissolved in each reactor thermal cycle. The allowable peak stress and FAD criteria for DHC initiation used in the paper for BPF and DFF structural analyses suppose the onset of hydride ratcheting condition.

3. STRESSES EVALUATION PROCEDURE

3.1 Assessment of bearing pad fretting flaw total hoop stresses by FEA

The increasing of deuterium/hydrogen in the pressure tubes becomes a structural integrity problem when the flaws are initiated at the rolled joint zones pressure tubes, as long as in these locations the pickup of hydrogen is in excess of the rest of tube. In figure 2 is depicted the profile of deuterium concentration along the pressure tube as result of corrosion process during normal operating conditions after 17 hot years [18]. It turns out that at rolled joints the equivalent hydrogen concentration exceeds TSSD limits at referred to pressure tube ends temperature: TSSD (250C) ~30 ppm (inlet), TSSD (300C) ~ 60 ppm (outlet)

A bearing pad fretting flaw (BPF) was described by Scarth in [5]. The flaw has a maximum depth of 0.4 mm at a corner, and an unusually small corner radius of approximately 20 μm. We will suppose a concurrent BPF for modeling located in pressure tube end with high hoop residual stresses. It must be note that the axial stresses of the pressure tube are smaller and structural integrity assessment are irrelevant in the axial direction.

An example of the structural assessment for bearing pad fretting flaws (BPF) was performed by D.A.Scarth, D.H.B. Mok and G.W. Newman in [4]. The main features of the assessment methodology were pointed out.

Connected with the stress analysis mentionable is fact the total hoop stress it will be consider the sum of two components: a hoop stress component resulted from internal pressure σ_{hp} of cooling agent and a residual hoop stress σ_{hr}:

$$\sigma_h = \sigma_{hp} + \sigma_{hr} \tag{2}$$

The nominal hoop stress from equation 2 will be amplified by a concentrator (flaw):

$$\sigma_{\max} = k \cdot \sigma_h \tag{3}$$

The values of stress concentrator factor *k* are known for particularly geometry and load conditions [4]. In the present paper the stress concentrator for a modeled BPF will be determined from FEA with FEA-Flaw computer code for stresses resulted from internal pressure and its value obtained will be applied for total hoop stresses at flaw.

In order to evaluate the DHC initiation potential at the analyzed BPF the allowable peak-flaw-tip stress criterion in the hydride ratcheting conditions [5] will be used.

3.2 Assessment of debrise fretting flaws in accordance with FAD-iDHC

The methodology to describe DHC initiation by means the failure assessment diagrams was developed by D. A. Scarth and T. Smith [9, 10]. These failure assessment diagrams could be designated with acronym FAD-iDHC (**F**ailure **A**ssessment **D**iagrams for **i**nitiation of **D**elayed **H**ydride **C**racking). A process-zone methodology was used to develop failure diagrams so the geometry dependence of the Failure Assessment Curves was minimized. The authors [9,10] have developed blunt notch failure assessment diagrams, such as used in the R6 procedure [19], although the diagram co-ordinates have different physical meanings. In the conventional R6 format for flaws like cracks, the K_r axis is the ratio of the applied stress intensity factor K divided by the fracture toughness K_c. In the FAD-iDHC for blunt flaws in hydride ratcheting conditions, the vertical axis K* is the ratio of applied peak flaw-tip stress, σ_p , calculated on an elastic bases, divided by the predicted threshold peak stress for DHC initiation at a deep flaw,σ_{p^*}:

$$K^* = \frac{\sigma_p}{\sigma_{p^*}} \tag{4}$$

The horizontal axis L_r from conventional R6 format was replaced with L* coordinate defined as:

$$L^* = \frac{\sigma_n}{p_c} \tag{5}$$

where σ_n is the applied nominal stress and p_c is the threshold stress for DHC initiation at a planar surface

An improved Mode I Failure Assessment Diagram based on more accurate threshold peak stress for deep flaw was developed by D.A. Scarth and T. Smith in [10]. In resume, we draw off the final form of K*-L* failure assessment curves with co-ordinate axis from [10]:

$$K^* = \frac{1+\frac{\theta(\lambda+2\cdot\theta)}{1+\theta}}{1+\frac{\theta(1.14+2\cdot\theta)}{1+\theta}} \tag{6}$$

$$L^* = \frac{1+\frac{\theta(\lambda+2\cdot\theta)}{1+\theta}}{1+2\cdot\sqrt{\frac{a}{\rho}}} \tag{7}$$

with:

$$\theta = \frac{K_{IH}}{p_c\cdot\left(\sqrt{\pi\rho}\right)} \tag{8}$$

$$\lambda = 0.81\cdot\sqrt{\frac{\rho}{h}} \tag{9}$$

$$h = \frac{\rho\left[1+0.5\sqrt{\frac{\rho}{a}}\right]}{2\left[1+\frac{3}{4}\sqrt{\frac{\rho}{a}}\right]} \tag{10}$$

K_{IH} – the isothermal threshold stress intensity factor for onset of DHC from a sharp crack, ρ – root radius at the blunt flaw-tip, a- the flaw depth

The assessment points (K^*_0 si L^*_0) will be generate for given ration a/ρ of the blunt flaw [10] from Eqs. 11, 12:

$$K_0^* = \frac{\frac{\sigma_p}{p_c}}{1+\frac{\theta(1.14+2\cdot\theta)}{1+\theta}} \tag{11}$$

$$L_0^* = \frac{\sigma_n\cdot k\left(\frac{a}{\rho};\frac{a}{t}\right)}{p_c\cdot k\left(\frac{a}{\rho};\frac{a}{t}=0\right)} \tag{12}$$

with $k\left(\frac{a}{\rho};\frac{a}{t}\right)$ - elastic stress concentration factor and *t* wall thickness of the pressure tube

DHC initiation is predicted to not occur when the assessment point of a blunt flaw lies below the failure assessment curve. In the present paper an example of DFF assessment will be performed in accordance with both allowable peak-flaw-tip stress and FAD-iDHC criteria in the hydride ratcheting conditions. The elastic stress concentration factor will be inferred from stress-strain analyses by means Finite Element Analysis performed on 3D blunt flaw model.

4. EXAMPLE OF STRUCTURAL INTEGRITY ASSESSMENTS

4.1 The BPF assessment based on allowable peak stress criterion

In Figure 3 are shown both sketch of models for a bearing pad fretting flaw and a debrise fretting flaw. For FEA a blunt flaw 3 D sketch that models a bearing pad fretting flaw (BPF) located on inner surface of the pressure tube was used with the main geometric characteristics: flaw depth: a= 0.4 mm; flaw length: 2c= 30 mm; minimum root radius: ρ=0.1mm.

The BPF model was considered on the inner surface of pressure tube in two internal pressurized cases of coolant agent: P_{int}= 10 MPa and P_{int}= 10 MPa. The Finite Element Analyses of stress-strain behavior were performed with FEA-Flaw computer code using Young's modulus by E=95 GPa and Poisson's ratio was ν=0.4. The considered residual stresses values were in the 50 MPa - 300 MPa range.

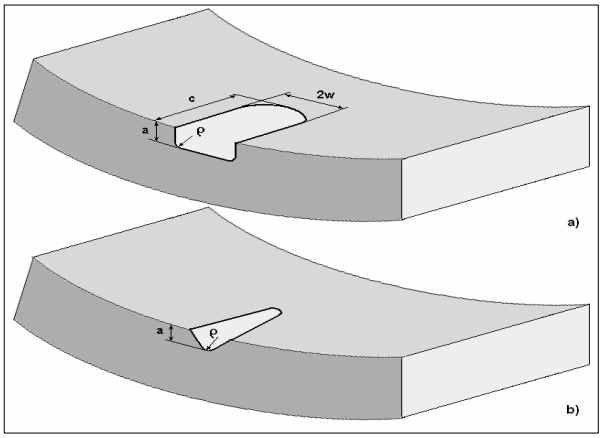

Figure 3. Models of BPF (a) and DFF (b)

The following main steps are performed for assessment:

- the nominal hoop stress σ_{hp} by FEA is obtained for a determinate internal pressure of coolant agent;
- the maximum hoop stress at flaw-tip σ_{hmax} is obtained by FEA;
- the elastic stress concentration factor is inferred by

$$k = \frac{\sigma_{h\max}}{\sigma_{hp}} \tag{13}$$

- the hoop residual stresses σ_{hr} get values in mentioned range ;
- the maximum residual stresses at flaw-tip are inferred by

$$\sigma_{hr\max} = k.\sigma_{hr} \tag{14}$$

- the total maximum hoop stresses at flaw-tip are inferred by

$$\sigma_{t\max h} = \sigma_{h\max} + \sigma_{hr\max} \tag{15}$$

- the stresses values resulted from Eq.15 are compared with threshold peak-flaw-tip stress σ_{TH} characteristic to designated root radius of BPF.

The Figure 4 shows the hoop stresses for same loading around the blunt BPF.

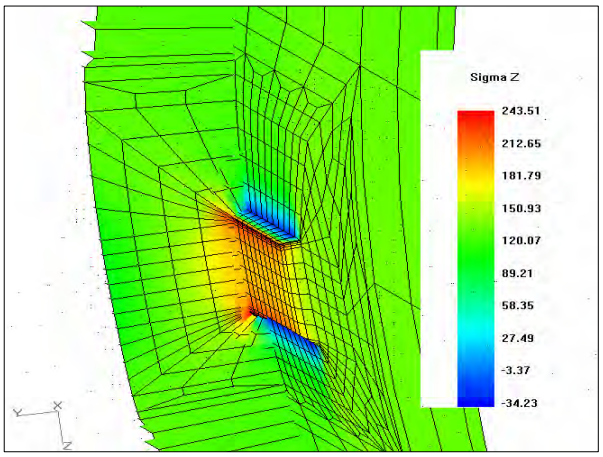

Figure 4. The hoop stress field at bearing pad flaw (FEA) (Pint=10 MPa)

The Table 1 contains the stresses from FEA and also total maximum hoop stresses values by counting residuals stresses and its comparisons with threshold peak-flaw-tip stress, σ_{TH}, in order to assess the DHC initiation occurrence.

Table 1 The DHC initiation assessments for a BPF model with ρ=0.1mm

P_{int} (MPa)	σ_{hp} MPa (FEA)	σ_{hmax} MPa (FEA)	k (Eq.13)	σ_{hr} MPa	σ_{hrmax} MPa (Eq.14)	σ_{tmaxh} MPa (eq.15)	Obs σ_{TH}=785MPa [5]
10	134	243	1.81	50 100 200 300	90 181 362 542	333 424 605 785	$<\sigma_{TH}$ $<\sigma_{TH}$ $<\sigma_{TH}$ $=\sigma_{TH}$
11	148	268	1.81	50 100 200 300	90 181 362 542	358 449 630 810	$<\sigma_{TH}$ $<\sigma_{TH}$ $<\sigma_{TH}$ $>\sigma_{TH}$

As a conclusion from structural integrity analyses presented in Table 1 according to the threshold peak stress criterion, the DHC initiation for residual hoop stresses greater then 200 MPa will occur.

4.2 The DFF assessment by means FAD criterion for DHC initiation

In order to perform the stress-strain assessment by FEA of a debrise fretting flaw located on inner surface of pressure tube has been selected a model with the main characteristics: root radius ρ=0.2 mm, flaw depth a = 1mm. For a/ ρ=5 ratio a Failure Assessment Curve (FAC) for DHC initiation has been constructed. Later on the failure assessment DFF points were plotted on FAC.

The following main steps were accomplished to perform assessment of DHC initiation by means of the FAD criterion:

- the DFF model with main geometric characteristics located on inner surface of P/T has been sketched;
- the threshold stress of DHC initiation at a planar surface p_c was taken to be 450 MPa [9, 10];
- the isothermal threshold stress intensity factor for onset of DHC from a sharp crack K_{IH} was taken to be in the 1-30 MPa√m range;
- the coordinate K*-L* pair obtained values according to the Eqs. 6 and 7;
- the pair values obtained at step 4 are plotted in K*-L* format and envelope curve generated the Failure Assessment Curve (FAC);
- the σ_{hp}, σ_{hmax} stresses were obtained from Finite Element Analyses (FEA) with FEA-Flaw computer code and the k factor was calculated;
- the hoop residual stress σ_{hr} was taken to be in 50 MPa-100 MPa domain;
- the maximum values of hoop residual stresses was obtained by σ_{hmaxr} =k. σ_{hr};
- the total maximum hoop stresses at flaw-tip have been inferred by $\sigma_{t\max h} = \sigma_{h\max} + \sigma_{hr\max}$ and the maximum peak stress was taken to be $\sigma_{t\max h} = \sigma_p$ in Eq. 11;
- the total nominal stress was given by $\sigma_h = \sigma_{hp} + \sigma_{hr}$ and considered it as σ_n in Eq. 12;
- the assessment points (K^*_o-L^*_0 pair) from Eqs. 11 and 12 were displayed on FAC.

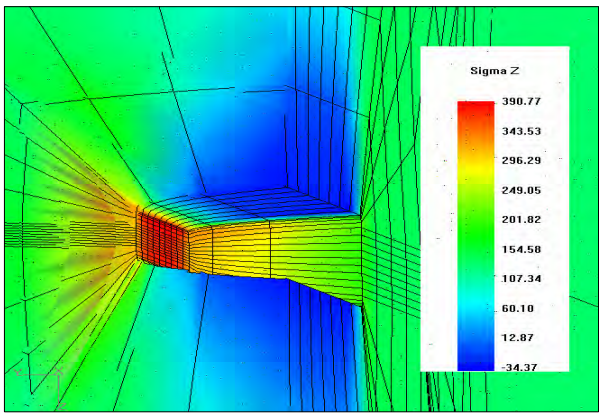

Figure 5. The hoop stresses around the debrise fretting flaw (FEA) (Pint=10 MPa)

The Figure 5 shows the hoop stresses for same loading around the blunt DFF.

The results from FEA and presented algorithm in the Table 2 are given. For comparison in the Table 2 are given also the threshold peak stress [5] corresponding to the modeled DFF.

Table 1 The FAD-iDHC assessments for a DFF model with ρ=0.2mm

P_{int} MPa	σ_{hp} MPa	σ_{max} MPa	k	σ_{hr} MPa	σ_{hrmax} MPa	σ_p MPa	σ_n MPa	K^*_0	L^*_0	Obs σ_{TH}=680MPa [5]
10	134	391	2.91	50	146	537	184	0.77	0.76	$\sigma_p<\sigma_{TH}$
10	134	391	2.91	100	291	682	234	0.98	0.97	$\sigma_p>\sigma_{TH}$

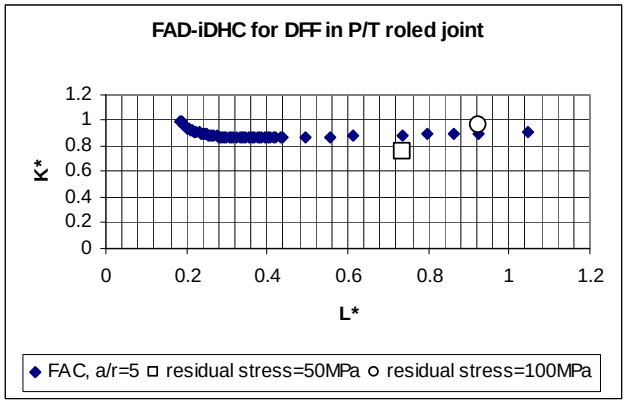

Figure 6. The FAD-iDHC for DFF accounting residual stresses

In Figure 6 is displayed the FAC for the considered blunt DFF together with the assessment points corresponding to 50 MPa and 100 MPa values of hoop residual stresses. In first case the FAD-iDHC criterion and threshold peak stress criterion predict the DHC did not occur and in second case both criteria predicted DHC initiation.

5. CONCLUSIONS

- Two blunt flaws type located on the inner surface of the CANDU pressure tubes were 3D modeled in order to perform DHC initiation assessment: the bearing pad fretting flaw (BPF) and the debrise fretting flaw (DBF);
- The stress-strain analyses were performed by means of FEA with FEA-Flaw computer code; later on the hoop stresses which appear at rolled joints location were considered;
- The methodology assessment were described for the threshold peak stress criterion and the Failure Assessment Diagram for initiation of DHC criterion;
- The threshold peak stress criterion was applied for BPF and both criteria for DFF; in the last case the criteria predictions are in a good agreement.

REFERENCES

1. IAEA-TECDOC-1037 “Assessment and management of ageing of major nuclear power plant components important to safety: CANDU pressure tubes”, , IAEA, August 1998
2. Shi, S.-Q., Puls, M.P. and Sagat, S., “Criteria of fracture initiation at hydrides in zirconium alloys II. Shallow notch”, *Journal of Nuclear materials*, 208 (1994), pp.243-250
3. Venkatapathi, S., Mehmi, A. and Wong, H. „Pressure Tube-to-End Fitting Roll-Expanded Joints in a CANDU PHWR”, *Proceedings of the International Conference on Expanded and Rolled Joint Technology*, Toronto, Ontario, Canada, September, 1993
4. Scarth, D.A., Mok, D.H.B., Newman, G.W., „Assessment of Bearing Pad Fretting Flaws in CANDU Zr-Nb Pressure Tubes”, in PVP-Vol.335, *Service Experience and Design in Pressure Vessels and Piping: Including High Pressure Technology*, ASME 1996
5. Scarth, D.A., Smith, E, „Developments in Flaw Evaluation Procedures for Zr-Nb Pressure tubes”, *Proceedings of the CANDU Owners Group Fuel Channel Seminar*, Toronto, Ontario, 15-16th , 2004
6. Shek, G.K., Resta Levi, M. “Experimental Data for the Assessment of DHC Initiation and Growth from Flaws in Zr-2.5%Nb Pressure Tubes, *Proceedings of the CANDU Owners Group Fuel Channel Seminar*, Toronto, Ontario, 15-16th , 2004
7. Sagat, S., Puls, M.P. and Shi, S.-Q. „Crack initiation at notches in Zr-2.5%Nb alloys”, *Materials Science and Engineering A176* (1994) 237-247

8. Scarth, D.A., Smith, T.,"The Effect of Plasticity on Process-Zone Predictions of DHC Initiation at a Flaw in CANDU Reactor Zr-2.5%Nb Pressure Tubes", *ASME Pressure Vessels and Piping Conference August 2002*, Vancouver , Canada
9. Scarth, D.A., Smith, T., "The use of Failure Assessment Diagrams to describe DHC initiation at a blunt flaw", PVP Vol.412, *Applications of Fracture Mechanics in Failure Assessment,* ASME 2000
10. Scarth, D.A., Smith, T., "Improved Failure Assessment Diagrams to describe DHC cracking initiation at a blunt flaw", PVP-vol. 462, *Application of Fracture Mechanics in Failure Assessment* -ASME 2003
11. Shi, S.-Q., Puls, M.P., "Criteria for Fracture initiation at hydrides in zirconium alloys I. Sharp crack tip", *Journal of Nuclear Materials* 208 (1994) pp. 232-250
12. Puls, M.P, "Assessment of ageing of Zr-2.5%Nb pressure tubes in CANDU Reactors", *Nuclear Engineering and Design 171* (1997) , pp.137-148
13. Venkatapathi, S., Hunter, T.A., Moan, G.D. "Residual Tresses in Fuel Channel Rolled Joints in CANDU PHWRS", *Practical Applications of Residual Stress Technology, Conference Proceedings*, Indianapolis, Indiana, USA, 15-17 May 1991
14. Coleman, C.E., "Cracking of Hydride-forming Metals and Alloys", *Comprehensive Structural Integrity, vol.6. Environmentally –Assisted Fracture*, 2003, Elsevier Ltd, pp.104-151
15. Price, E.G., "Introduction and Review", *Proceedings of the CANDU Owners Group Fuel Channel Seminar*, Toronto, Ontario, 15-16th , 2004
16. IAEA-TECDOC-1410, "Delayed hydride cracking in zirconium alloys in pressure tube nuclear reactors" *Final report of a coordinated research project 1998–2002, ,* October 2004
17. Eadie, R.L., Metzger, D.R., Leger, M. " The Thermal Ratcheting of Hydrogen in Zirconium-Niobium – An Illustration using Finite Element Modeling", *Scripta metallurgica et Materialia*, vol.29, pp. 335-340, 1993
18. Elmoselhi, M.B., Bahurmuz, A., " Predicting Deuterium Buildup in the rolled joint regions of Operating Pressure Tubes", *Proceedings of the CANDU Owners Group Fuel Channel Seminar*, Toronto, Ontario, 15-16th , 2004
19. BEGL, "R6/Revision 4 - Assessment of the Integrity of Structures Containing Defects", Barnwood, Published in the UK, British Energy Generation Ltd., 2001